X-ray absorption spectroscopy of vanadium dioxide thin films across the phase-transition boundary

Dmitry Ruzmetov,[1] Sanjaya D. Senanayake,[2] and Shriram Ramanathan[1,*]
[1]*School of Engineering and Applied Sciences, Harvard University, Cambridge, Massachusetts 02138, USA*
[2]*Chemical Sciences Division, Oak Ridge National Laboratory, Oak Ridge, Tennessee 37831, USA*
(Received 14 December 2006; revised manuscript received 21 February 2007; published 3 May 2007)

X-ray absorption spectroscopy (XAS) and x-ray photoemission spectroscopy of the V *L* edge and O *K* edge were performed on VO_2 thin films rf sputtered at various conditions. The spectra give evidence of the changes in the electronic structure depending on the film quality. XAS of the O *K* edge shows a decrease of the spacing between $3d_\pi$ and $3d_\sigma$ bands by 0.8 eV with concurrent broadening of both bands for the sample sputtered at lower substrate temperature and consequently having more polycrystalline and disordered character. $3d_\sigma$ band position appears to be more sensitive to the sample quality, indicating that the cation-ligand interaction is mostly affected likely due to the distortion of the local O coordination surrounding a V ion. The observed variation of the spectra in films of different morphologies may reflect the changes of the density of states responsible for the considerable variation of the metal-insulator transition (MIT) properties reported for VO_2 thin films synthesized at different conditions. The study of the temperature dependence of the XAS spectra including repeated measurements across the MIT revealed both reversible and irreversible V *L*-edge and O *K*-edge changes. The thermal cycling of the VO_2 films through the MIT shows irreversible shifts of the conduction bands toward lower photon energies apparently caused by the sample deterioration due to the lattice transformations at the MIT. The signature of a phase transition in a VO_2 film at MIT temperature (T_{MIT}) is clearly seen in the XAS O *K*-edge spectra which show reversible switches of the $3d_\pi$ and $3d_\sigma$ bandwidths by approximately 20% depending on the sample being above or below T_{MIT}.

DOI: 10.1103/PhysRevB.75.195102 PACS number(s): 71.30.+h, 78.70.Dm, 79.60.−i, 73.20.At

I. INTRODUCTION

Vanadium dioxide is a strongly correlated electron compound which exhibits a dramatic metal-insulator transition (MIT).[1] Above the transition temperature T_{MIT}=67 °C, VO_2 has tetragonal rutile lattice structure which transforms to the monoclinic with unit cell doubling below T_{MIT}. To explain the origin of the MIT in VO_2, early theoretical models suggested that the unit-cell distortion and strong electron-lattice coupling caused a Peierls-type transition.[2] Noticing the importance of electron-electron correlations in VO_2 gave rise to models ascribing the MIT to be of the Mott-Hubbard type.[1] The transition has an impressive scale with over 4 orders of magnitude resistivity change[3] and strong suppression of optical transmission.[4] Recent reports on short switching times,[5] as well as the possibility to induce the MIT by an electric field,[6,7] added interest in the effect from theoretical and practical perspectives. However, there is still no general agreement whether the primary cause of the MIT is the structural change due to unit cell distortion[8,9] or electron-electron correlations.[10,11]

X-ray absorption spectroscopy (XAS) has proven to be a valuable tool to study the unoccupied conduction bands of VO_2 crystals above and below T_{MIT} and improve the understanding of this system.[12,13] Using these materials in nanoscale integrated device technologies could well require employing thin VO_2 films. Yet there are scarce XAS data for thin VO_2 films. The MIT characteristics vary significantly for thin films and bulk crystals, and for thin films prepared at different conditions.[3] Using XAS to relate this variation to the changes in the electronic structure should provide a bridge between macroscopic observables of the MIT and microscopic models describing the transition.

In this paper, we systematically study the XAS and x-ray photoemission spectroscopy (XPS) spectra of the V *L* edge and O *K* edge of VO_2 thin films. Besides providing detailed data on the VO_2 absorption edges, the XAS study presented below addresses the following aspects. First, we investigate the spectra of VO_2 thin films specifically looking into variations depending on the differences in the film preparation conditions. Such data are important in order to understand the origin of observed large variations in MIT characteristics from one sample to another. Secondly, we investigate the evolution of XAS spectra with thermal treatment looking particularly for irreversible changes occurring after multiple thermal cycles. This issue has been so far poorly covered in the literature to our knowledge. Our results provide insights into the origin of hysteresis during the transition.

II. EXPERIMENTAL DETAILS

Thin films of VO_2 were deposited on Si/SiO_2 (native oxide) substrates by means of rf sputtering of VO_2 target for 30 min at a rate of 19 Å/min at total pressure of 8 mTorr. Sample 1 was deposited at the substrate temperature T_{subs} =300 °C in pure Ar, and samples 2 and 3 were deposited simultaneously at T_{subs}=500 °C in Ar(99.2%)+O_2(0.8%) with subsequent annealing at 500 °C for 20 min in the same gas mixture. The resulting film thickness was measured by means of grazing incidence x-ray reflection analysis to be 57 nm. X-ray diffraction and grazing incidence reflection measurements were done on a Scintag 2000 diffractometer using Cu $K\alpha$ radiation.

XAS (in our case the near edge x-ray absorption fine structure technique) measurements and XPS were performed

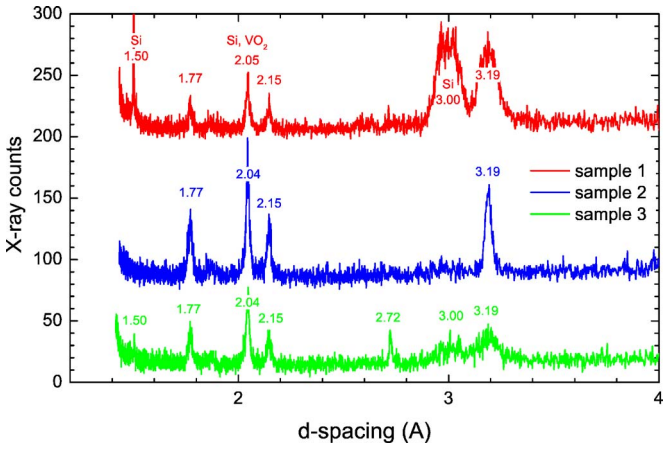

FIG. 1. (Color online) Cu $K\alpha$ θ-2θ x-ray diffraction spectrum of VO_2 films. The spectra are displaced vertically for clarity. Samples 2 and 3 are synthesized simultaneously at identical conditions. The shown XRD spectrum of sample 3 was measured after the thermal cycling involved in the XAS measurements displayed in Figs. 6 and 7.

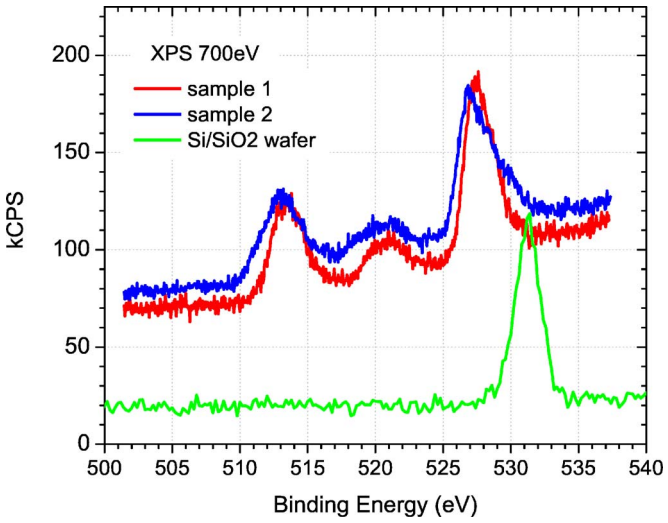

FIG. 2. (Color online) XPS spectrum of the O 1s and V $2p_{3/2}$ and V $2p_{1/2}$ edges for samples 1, 2, and blank Si/SiO_2 substrate.

at the U12a line of the National Synchrotron Light Source in the Brookhaven National Laboratory. The XAS measurements are done using a partial Auger yield detector that uses an energy deflection grid at the front of the detector biased with a voltage of −200 V to rule out any secondary electrons in the XAS signal. XPS was done at a constant photon energy of 700 eV. X-ray beam size was approximately $1.5(v) \times 7(h)\text{mm}^2$ with the intensity on the order of 2×10^{11} photons/s. The sample normal was at approximately 35° to the beam direction. The photon E-field polarization was in the plane defined by the line of incidence and a normal to the VO_2 film. The comparison of O K edge measured on a blank Si/SiO_2 substrate with published O K-edge data on SiO_2 (Refs. 14 and 15) was used to calibrate the absolute value of the photon energy in the XAS measurements. The presented XAS data are normalized to the maximum of intensity which is scaled to unity. The normalized spectra are shifted along the intensity axis for clarity. XPS of the Si $2p$ edges in Si (99 eV) and SiO_2 (103 eV) measured on a blank Si/SiO_2 substrate was used to correct for the instrumental shift in the XPS data.

III. RESULTS AND DISCUSSION

X-ray diffraction (XRD) $\theta-2\theta$ analysis with Cu $K\alpha$ radiation of the three samples revealed that all three samples show VO_2 lines at lattice spacings $d=3.19, 2.15, 2.04$, and 1.77 Å, besides Si substrate lines $d=3.00, 2.05$, and 1.50 Å (Fig. 1). Si lines were determined by measuring a blank Si substrate. VO_2 lines were identified by comparing with published data.[16,17] These x-ray results confirm that rf sputtering from a VO_2 target (compared to typical reactive V sputtering) can be used to produce phase pure VO_2 phase.

We used the Scherrer formula[18,19]

$$t = \frac{0.9\lambda}{B \cos \theta_B} \tag{1}$$

to extract the estimates of the grain sizes of the VO_2 films from the measured XRD data in Fig. 1. In the formula, t is the crystallite size, defined as the cube root of the crystallite volume, $\lambda = 1.542$ Å—Cu $K\alpha$ radiation wavelength, B is the width of the diffraction peak measured in radians from the counts vs 2θ plot, and θ_B is the Bragg angle. We applied the formula to the strongest VO_2 peaks ($d=3.19, 2.15$, and 1.77 Å) that do not overlap with substrate peaks. B and θ_B were estimated from Lorentzian fitting to individual peaks. The calculated grain sizes averaged over all three peaks for each sample are 14, 20, and 13 nm for samples 1, 2, and 3, respectively.

Smaller grain size and larger amount of disorder have been reported for samples reactively sputtered at lower substrate temperatures.[3,20] We found similar tendency in our sputtering technique manifested by broader and weaker XRD lines of sample 1 versus sample 2 implying that sample 2 has better crystalline quality. Sample 3 was synthesized along with sample 2 but underwent thermal cycling during the XAS measurements. Broader and weaker VO_2 XRD lines of this sample vs sample 2 concurrently with the appearance of a new unidentified line at $d=2.72$ Å were observed after the cycling. The grain size estimates evidence the breakage of the grains into the smaller ones during the temperature-dependent XAS measurements. Even though thin films are considered to better withstand the stresses due to the lattice transformation at the MIT compared with bulk crystals, there was apparently some lattice deterioration in sample 3 due to the multiple passing through the transition and possibly the appearance of the traces of a new stoichiometric VO_x phase. This is further discussed in this paper.

Room-temperature XPS data for the samples 1, 2, and a bare Si/SiO_2 (native layer) substrate are shown in Fig. 2. The photoemission spectra are taken in the range of the binding energies of the core levels V $2p_{3/2}$, V $2p_{1/2}$, and O 1s. The results of the analysis of the XPS data using FITXPS software[21] are summarized in Table I. Sample 2 has the same binding-energy peak positions as sample 1 but with considerably broader lines. It is interesting to note also the skewed character of the XPS spectrum of this sample as opposed to the more symmetrical peaks of sample 1.

TABLE I. XPS core-level peak positions and widths (in eV) for samples 1 and 2.

	V $2p_{3/2}$		V $2p_{1/2}$		O 1s	
	BE	FWHM	BE	FWHM	BE	FWHM
Sample 1	513.4	2.6	520.8	2.9	527.4	2.5
Sample 2	513.4	3.3	520.8	4.0	527.4	3.4

In order to understand the XAS spectra, Fig. 3 gives the band structure near the Fermi level based on Goodenough's classification[2] taking into account the new XAS data, showing that the upper $d_{\|}$ band in the insulating phase actually reaches above the π^* band.[12,22] XAS results at room temperature for samples 1 and 2 are given in Fig. 4. V L edge (transitions from $2p$ to $3d$ levels) has two pronounced maxima at 517 and 524 eV which roughly correspond to the electron excitations from spin-orbit split levels $2p_{3/2}$ and $2p_{1/2}$, respectively. The final states of the transition are the unoccupied levels of the hybridized V $3d$ and O $2p$ orbitals. The selection rules for the electron transition during photon absorption require $\Delta l = \pm 1$, so that the V L-edge absorption describes the d-projected unoccupied density of states (UDOS) of the valence levels (perturbed due to the presence of the core hole created by the absorption). Correspondingly, O K-edge absorption depends on the p-projected UDOS. This selectivity of the XAS results in the V L-edge transition mainly into $d_{\|}$ orbitals,[23] whereas O K edge contains signatures of all three bands near the Fermi level—π^*, σ^*, and $d_{\|}$.[22]

We first note from Fig. 4(a) that the V-edge main peak maxima positions (presumably from $3d_{\|}$ band) of the different VO_2 films are the same. An obvious difference of the spectra is the presence of a shoulder at 515 eV for sample 2 that is not readily seen in sample 1. The satellite shoulder is absent in the powder VO_2 and polycrystalline VO_2 films on Si_3N_4,[24] whereas in single VO_2 crystals, the shoulder is even stronger pronounced than for our sample 2.[12] The published electron-diffraction data from VO_2 samples reactively sputtered at 300 °C (and lower temperatures) showed circular diffraction pattern characteristic to polycrystalline samples, whereas samples sputtered at 400 °C exhibited single crystal pattern.[20] Thus, sample 2 sputtered at 500 °C is expected to have a highly textured crystalline character. Indeed, its V-edge spectrum shows the shoulder at 515 eV in accord with the XAS data on single crystals.[12] The more disordered sample 1 has the spectrum characteristic to polycrystalline and powder VO_2. The resolution of the data in Fig. 4(a) allows for more detailed analysis. There is a small satellite at 516.9 eV near the $p_{3/2}$ peak even for sample 1. It shifts away from the $p_{3/2}$ peak maximum by 1.9 eV in sample 2. One can see the movement of a satellite by 0.7 eV for the $p_{1/2}$ peak as well. We conclude that there are satellite lines in the V-edge

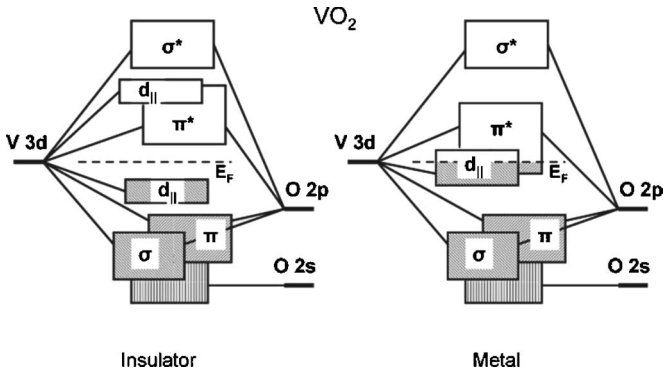

FIG. 3. Band structure of VO_2 near Fermi level in metallic and insulating phases as the result of the hybridization of V and O orbitals based on Goodenough's description (Ref. 2).

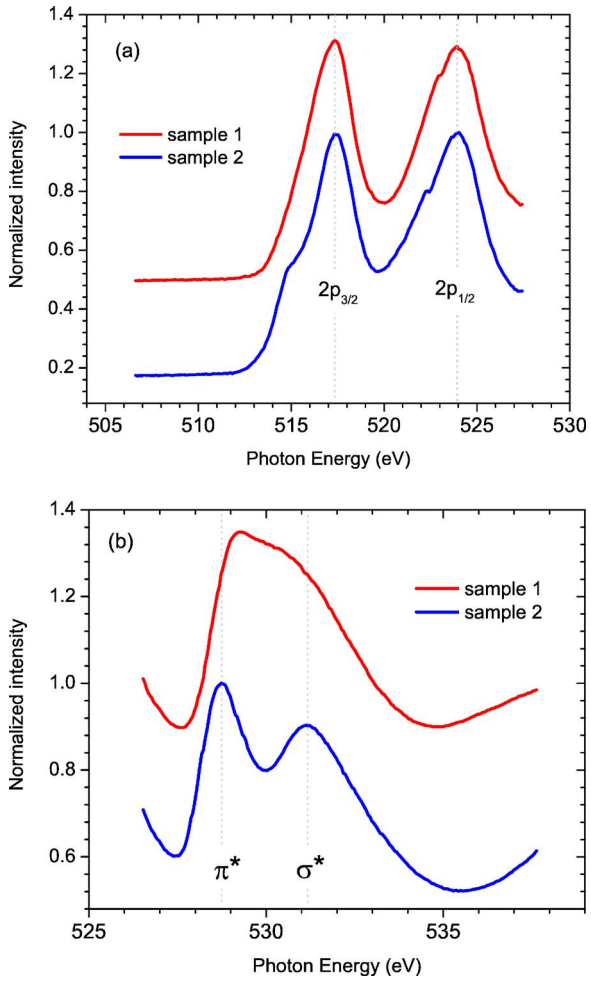

FIG. 4. (Color online) Room-temperature XAS data for samples 1 (sputtered at 300 °C) and 2 (500 °C). (a) V edge and (b) O edge. V and O edges were measured separately since their peak intensities were different. The spectra are normalized to the maximum of intensity and displaced vertically for clarity.

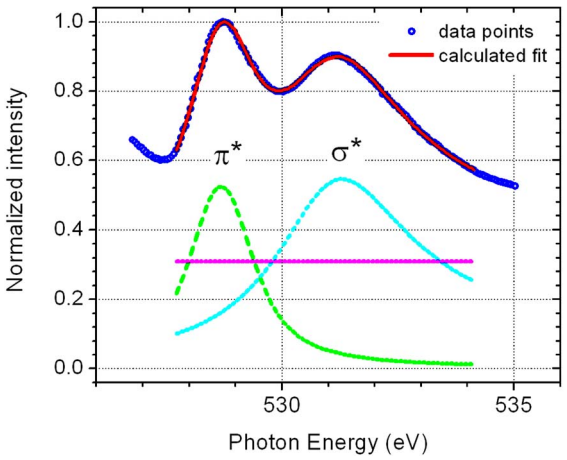

FIG. 5. (Color online) An example of fitting to the measured XAS O *K*-edge spectrum for sample 2 at room temperature using FITXPS software package (Ref. 21). The calculated line goes within the width of the data marks. Below are three components of the calculated line: a constant background line and 2 peaks of the Doniach-Sunjic line shape (Ref. 26) convoluted with a Gaussian. The fitting results are given in Table II.

spectra which move toward merging with main peaks with increasing disorder of the film. It is interesting to compare the V 2*p* spin-orbit splitting derived from XPS (7.4 eV, Table I) and XAS V edge [6.5 eV, Fig. 4(a)]. The 0.9 eV disparity may be due to the self-energy effects:[25] the final state of the excited electron is different in the XAS and XPS processes, then the interaction of the excited electron with its surroundings modifies the density of states in a different degree in XAS and XPS.

There is a considerable difference between samples 1 and 2 in their O *K*-edge spectra [Fig. 4(b)]. Each spectrum consists of a prominent doublet corresponding to the transitions from the O 1*s* level to the π^* and σ^* bands (Fig. 3). FITXPS software package[21] was used to extract the positions and widths of the peak components in the XAS O *K*-edge doublets. The doublets were fitted with the algebraic sum of two peaks and a constant background line. The line shape of each peak employed in the software is a numerical convolution of an analytical Doniach-Sunjic line shape[26] with a Gaussian. The asymmetry of the peak was taken into account with the Doniach-Sunjic parameter α, where $\alpha=0$ corresponds to a symmetric Lorentzian line shape. The Gaussian represents the broadening due to the experimental instrument function and possible broadening of the core-electron line shape due to thermal vibrations and static disorder. A typical example of the spectra fitting is given in Fig. 5. The fitting results of the O *K*-edge spectra are summarized in Table II. We see in the table that the spacing (Δ) between π^* and σ^* bands of samples 1 and 2 [extracted from the raw data in Fig. 4(b)] decreases by 0.8 eV in the more disordered sample 1 which is accompanied with line broadening. Such changes in the band structure may explain dramatic differences in the MIT properties of VO_2 thin films depending on the sample preparation conditions.[3]

Figure 6 shows the temperature dependence of the V and O edges of sample 3. The initial temperature is 32 °C in both graphs. The V *L*-edge peak maxima move continuously toward lower photon energies during thermal cycling with the total shift of 0.55 eV for the lower band (V $p_{3/2}$, initially at 518 eV). Most of the shift (0.45 eV) occurs upon the first heating cycle from 32 to 113 °C. Subsequent cooling down to 0 °C and heating up to 110 °C move the peak further by 0.1 eV. The band shifts at temperatures above and below T_{MIT} in VO_2 probed by XPS and XAS have been reported earlier.[22,27] However, the absence of the thermal cycling data in the literature did not allow us to judge whether the changes were permanent or could be relaxed back to the initial state depending on the temperature. *Our data allow one to conclude that there are permanent band-structure changes which are likely due to the distortions during the phase transition involving the lattice transformation*. Such distortions, for example, may cause the breakage of the sample into smaller grains reducing the strain in the lattice which would be reflected in the band structure. This lattice deterioration scenario is supported by the x-ray-diffraction data (Fig. 1), showing that the spectrum of sample 3 after the thermal cycling resembles sample 1 with broader and weaker peaks due to smaller grain size and higher disorder. This deterioration apparently saturates since the second heating of the sample through the MIT causes the smaller V $p_{3/2}$ peak shift of 0.1 eV.

Similar behavior is exhibited in the O *K* edge. Figure 7(a) illustrates how the position of π^* band peak moves upon the thermal treatment of sample 3. The peak does not shift (within the instrument resolution of ~0.1 eV) for first measurements below T_{MIT} and drops to smaller photon energies upon the first cross of the MIT. Second *T* raise through the MIT causes a smaller drop. We see that the changes in the

TABLE II. XAS O *K*-edge analysis for samples 1, 2, and 3 (♯). Given are line positions extracted from the data in Figs. 4 and 6 for bands π^* and σ^* (PE, eV), their widths (FWHM, eV), line spacing between π^* and σ^* (Δ, eV), relative intensities (π^*-line height/σ^*-line height, $h_{\pi/\sigma}$), and temperature of the measurement (*T*, °C).

♯	*T*	π-PE	π-FWHM	σ-PE	σ-FWHM	Δ	$h_{\pi/\sigma}$
1	26±5	528.9	1.9	530.4	5.0	1.5	1.2
2	26±5	528.7	1.7	531.0	4.4	2.3	1.0
3	109±1	528.8	1.3	531.2	3.6	2.4	0.8
p[a]	RT	528.8	1.8	531.0		2.2	

[a]Powder VO_2 data taken from Ref. 25.

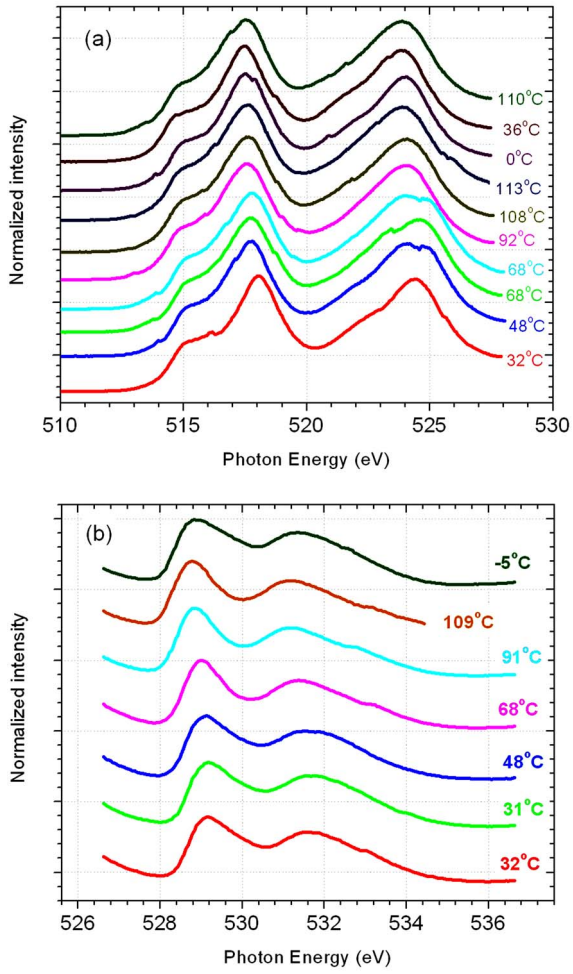

FIG. 6. (Color online) Temperature dependence of the XAS spectra for sample 3. (a) V edge and (b) O edge. The initial temperature is 32 °C. We repeated the scan in the V edge at 68 °C near the T_{MIT} after the delay of 1 h and 40 min. The first two scans in the O edge at the same temperature are given to judge on the reproducibility. The spectra are normalized to the maximum of intensity and displaced vertically for clarity.

XAS spectra again are not reversible and saturate upon thermal cycling. It is worthwhile to consider the oxidation state change of VO as a reason for the observed XAS spectra shifts. The study by Chen *et al.*[28] showed that V $2p_{1/2}$ and V $2p_{3/2}$ edges move by 0.68 eV per oxidation state for various vanadium oxides. Then, the sample heating could cause the loss of oxygen and transformation to the lower oxidation state, such as V_2O_3. In that case, however, the observed $p_{3/2}$ peak shift of 0.55 eV would correspond to almost complete oxide phase change to V_2O_3 which should be reflected in the XAS line shapes,[28] especially in the O edge. Significant changes in the line shapes are not observed, however, as illustrated in Fig. 6. Also, even though the appearance of an extra peak at d=2.72 Å implies the appearance of a trace of a substoichiometric VO_x phase, all the VO_2 peaks in the x-ray diffraction data are still present for sample 3 (Fig. 1), indicating that the VO_2 phase is mainly preserved. Therefore, changes of film texture and quality are more likely to be the reasons of the observed drifts of the band positions upon thermal cycling.

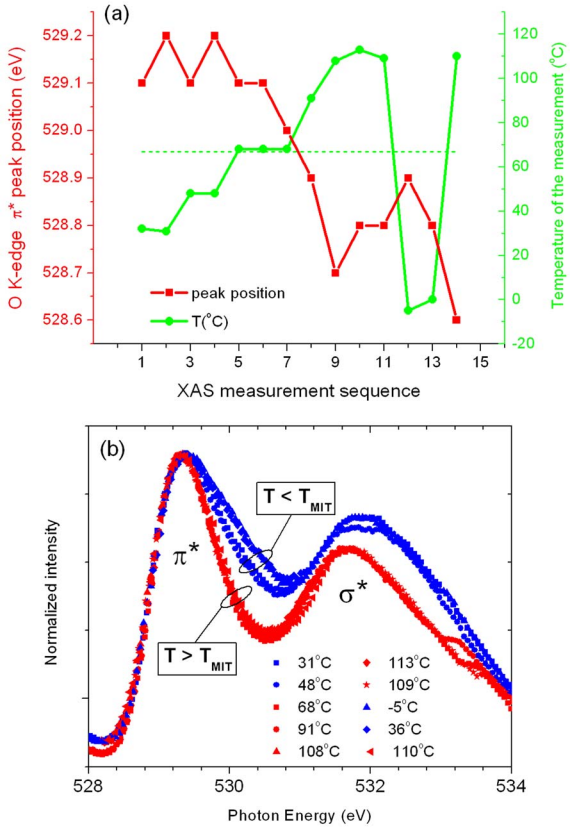

FIG. 7. (Color online) (a) Displacement of the O K-edge π^*-peak maximum during measurements. The peak shifts toward lower photon energy every time the sample is heated up through the T_{MIT}. T_{MIT} is displayed by a dashed line. (b) The line broadening in the O K edge. Spectra are shifted to coincide at the maximum of intensity. Two groups of spectra are marked by color (online) and loops depending on the sample temperature being below or above T_{MIT} (≈67 °C). Two distinct widths of the π^* band below and above the MIT are obvious.

The V-edge spectra in Fig. 6 show another interesting feature around the transition temperature—the doubling of the $2p_{1/2}$ band at 524 eV. The splitting disappears at higher temperatures so that commonly reported data well above and below T_{MIT} would not show the effect.

Besides permanent peak position shifts, O K-edge spectra reveal another temperature dependence which is reversible with temperature. Figure 7(b) displays O K-edge spectra for various temperatures normalized to the peak heights and shifted in the photon energy so that their first maxima coincide. All runs done at $T<T_{MIT}$ are plotted in blue, and runs at $T>T_{MIT}$ are red. We see a distinct switch of the width of the π^* band depending on whether the sample is below or above T_{MIT}. Detailed analysis[21] shows that both π^* and σ^* bands broaden below the transition, while their spacing remains the same (samples 2 and 3 in Table II). There is no obvious presence of the $d_{\|}$ band in the spectra which was observed in VO_2 single crystals for specific orientation of the photon polarization.[22] Even though there may be an indication of a line at 530.4 eV in the low-temperature curves, the $d_{\|}$ presence is obscured probably by the untuned polarization orientation or averaged away in the polycrystalline film.

Taking into account the symmetry of the orbitals in the compound can help interpret the O K-edge data summarized in Table II. π orbitals in VO_2 point in between the ligands (O ions) and σ orbitals are directed toward the ligand. Therefore, V-V interactions affect the π band more, whereas the σ band is influenced by the V-ligand configuration and the indirect V-O-V interaction. One can see that σ^* band moves considerably more than π^* band for different quality samples (Table II, samples 1 and 2). This can be taken as evidence that the variation in such samples comes mostly from the distortion of the O octahedra with respect to the V ions. In this case, we note that the change in the oxygen coordination of the V ions also results in the change of the π^*-σ^* spacing Δ. Interestingly, Δ remains the same upon crossing of the MIT (samples 2 and 3). Even though both bands drift upon thermal treatment of the sample, this change is irreversible so that it is not connected with the MIT. Then, the unaffected π-σ spacing probably indicates that the V-V pairing at the MIT (resulting in the unit cell doubling and lattice transformation from tetragonal to monoclinic) is not accompanied with O octahedra distortion.

In conclusion, we discussed detailed XAS and XPS spectroscopy results on VO_2 thin films synthesized under various conditions. The spacing between π^* and σ^* bands in the XAS O K edge decreases by 0.8 eV mainly at the expense of the shift of the σ^* band in the sample with smaller grain size and higher disorder. This is also accompanied by approximately 13% broadening of the spectral lines. The decrease in spacing is ascribed to the distortion of O coordination surrounding the V ions. The higher crystalline quality of VO_2 in sample 2 versus more disordered sample 1 is manifested in the XAS V edge by the appearance of a distinct shoulder in the $2p_{3/2}$ line displaced by 2.2 eV from the main peak. Over 20% width changes of the core V $2p$ and O $1s$ levels are found in the XPS spectra for different quality thin films. The XAS study of the temperature dependence across the MIT of a VO_2 film reveals permanent shifts of the V- and O-edge bands toward lower photon energies. The main part of the shift occurs upon crossing the MIT from low T to high T phase. This is taken as evidence that the shift originates from the film texture deterioration due to the lattice transformation at the phase transition. The signature of a phase transition in the VO_2 film at T_{MIT} is clearly seen in the XAS O K-edge spectra which show reversible switches of the π^* and σ^* bandwidths by approximately 20% depending on the sample being above or below T_{MIT}.

ACKNOWLEDGMENTS

This work was supported primarily by the NSF-SIA Supplement to the Nanoscale Science and Engineering Initiative under NSF Award No. PHY-0601184. SDS and the U12a beamline are supported by the Division of Chemical Sciences, Geosciences, and Biosciences, Office of Basic Energy Sciences, U.S. Department of Energy, under Contract No. DE-AC05-00OR22725 with Oak Ridge National Laboratory, managed and operated by UT-Battelle, LLC. Use of the National Synchrotron Light Source, Brookhaven National Laboratory, was supported by the U.S. Department of Energy, Office of Science, Office of Basic Energy Sciences, under Contract No. DE-AC02-98CH10886.

*Electronic address: shriram@seas.harvard.edu

[1] A. Zylbersztejn and N. F. Mott, Phys. Rev. B **11**, 4383 (1975).
[2] J. B. Goodenough, J. Solid State Chem. **3**, 490 (1971).
[3] P. Jin, K. Yoshimura, and S. Tanemura, J. Vac. Sci. Technol. A **15**, 1113 (1997).
[4] H. Wang, X. Yi, S. Chena, and X. Fua, Sens. Actuators, A **122**, 108 (2005).
[5] B.-G. Chae, H.-T. Kim, D.-H. Youn, and K.-Y. Kang, Physica B **369**, 76 (2005).
[6] P. P. Boriskov, A. A. Velichko, A. L. Pergament, G. B. Stefanovich, and D. G. Stefanovich, Tech. Phys. Lett. **28**, 406 (2002).
[7] H.-T. Kim, B.-G. Chae, D.-H. Youn, G. Kim, K.-Y. Kang, S.-J. Lee, K. Kim, and Y.-S. Lim, Appl. Phys. Lett. **86**, 242101 (2005).
[8] R. M. Wentzcovitch, W. W. Schulz, and P. B. Allen, Phys. Rev. Lett. **72**, 3389 (1994).
[9] A. Cavalleri, T. Dekorsy, H. H. W. Chong, J. C. Kieffer, and R. W. Schoenlein, Phys. Rev. B **70**, 161102(R) (2004).
[10] T. M. Rice, H. Launois, and J. P. Pouget, Phys. Rev. Lett. **73**, 3042 (1994).
[11] M. S. Laad, L. Craco, and E. Muller-Hartmann, Phys. Rev. B **73**, 195120 (2006).
[12] M. Abbate, F. M. F. deGroot, J. C. Fuggle, Y. J. Ma, C. T. Chen, F. Sette, A. Fujimori, Y. Ueda, and K. Kosuge, Phys. Rev. B **43**, 7263 (1991).
[13] M. Haverkort, Z. Hu, A. Tanaka, W. Reichelt, S. Streltsov, M. A. Korotin, V. I. Anisimov, H. H. Hsieh, H.-J. Lin, C. T. Chen *et al.*, Phys. Rev. Lett. **95**, 196404 (2005).
[14] D. A. Muller, T. Sorsch, S. Moccio, F. H. Baumann, K. Evans-Lutterodt, and G. Timp, Nature (London) **399**, 758 (1999).
[15] Y. Yamashita, S. Yamamoto, K. Mukai, J. Yoshinobu, Y. Harada, T. Tokushima, T. Takeuchi, Y. Takata, S. Shin, K. Akagi *et al.*, Phys. Rev. B **73**, 045336 (2006).
[16] C. Griffiths and H. K. Eastwood, J. Appl. Phys. **45**, 2201 (1974).
[17] M. Israelsson and L. Kihlborg, Mater. Res. Bull. **5**, 19 (1970).
[18] B. D. Cullity, *Elements of X-ray Diffraction* 2nd ed. (Addison-Wesley, Reading, MA, 1978).
[19] J. I. Langford and A. J. C. Wilson, J. Appl. Crystallogr. **11**, 102 (1978).
[20] N. R. Mlyuka and R. T. Kivaisi, J. Mater. Sci. **41**, 5619 (2006).
[21] The FITXPS Version 2.12 (http://www.sljus.lu.se/download.html) software was used to analyze the XPS and XAS spectra. The XAS spectra were inverted in photon energy before fitting with the program.
[22] T. C. Koethe, Z. Hu, M. Haverkort, C. Schubler-Langeheine, F. Venturini, N. B. Brookes, O. Tjernberg, W. Reichelt, H. H. Hsieh, H.-J. Lin *et al.*, Phys. Rev. Lett. **97**, 116402 (2006).

[23] A. Cavalleri, M. Rini, H. H. W. Chong, S. Fourmaux, T. E. Glover, P. A. Heimann, J. C. Kieffer, and R. W. Schoenlein, Phys. Rev. Lett. **95**, 067405 (2005).
[24] A. Cavalleri, H. H. W. Chong, S. Fourmaux, T. E. Glover, P. A. Heimann, J. C. Kieffer, B. S. Mun, H. A. Padmore, and R. W. Schoenlein, Phys. Rev. B **69**, 153106 (2004).
[25] F. M. F. de Groot, M. Grioni, J. C. Fuggle, J. Ghijsen, G. A. Sawatzky, and H. Petersen, Phys. Rev. B **40**, 5715 (1989).
[26] S. Doniach and M. Sunjic, J. Phys. C **3**, 285 (1970).
[27] G. A. Sawatzky and D. Post, Phys. Rev. B **20**, 1546 (1979).
[28] J. Chen, C. Kim, B. Friihberger, B. DeVries, and M. Touvelle, Surf. Sci. **321**, 145 (1994).